Research Article

Chemical Review and Letters
journal homepage: www.chemrevlett.com
ISSN (online): 2645-4947 (print) 2676-7279

Molecular Dynamic Simulations and Quantum Chemical Studies of Nitrogen Based Heterocyclic Compounds as Corrosion Inhibitors on Mild Steel Surface

Fater Iorhuna[1, *], Abdulfatah Shehu Muhammad[1], Abdullahi Muhammad Ayuba[1], Nyijime Aondofa Thomas[2]

[1] *Department of Pure and Industrial Chemistry, Faculty of Physical Sciences, Bayero University, Kano, Kano-Nigeria.*
[2] *Department of Chemistry, Joseph Saawuan Tarkaa University, Makurdi, Benue, Nigeria*

ARTICLE INFO

Article history:
Received 7 June 2023
Received in revised form 3 July 2023
Accepted 15 July 2023
Available online 10 August 2023

Keywords:
Physisorption
quantum-chemical parameters
molecular dynamic simulation
binding energy
Fukui indices

ABSTRACT

Through the use of theoretical techniques, this study investigated the corrosion inhibition potentials of a few chosen nitrogen-based five membered ring heterocycles, such as 2-methyl-1H-imidazole (2MI), 2-methyl-oxazole (2MO), 2,4,5-trimethyl-thizole (2TT), and 3-methyl-4,5-dihydro-1H-pyrole (MPP), on the surface of mild steel. To determine the potentials of these compounds in corrosion inhibition and to suggest a mechanism for the process, quantum chemical parameters, Fukui indices, and quench molecular dynamic simulation approaches were used. The corrosion inhibition potentials of the examined compounds were discovered to be caused by the existence of numerous hetero atoms rich in n-electrons, pi-bonds, molecular shape, and charge distribution. The outcomes demonstrated that each molecule's adsorption or binding energy is negative and comparatively low, less than the ±100kcal/mol threshold. It has also been discovered that, depending on the parameters examined, the 2TT molecule may be more efficient in preventing corrosion on the Fe (1 1 1) surface. This is owing to the sp^3 sulfur heteroatom in its structure, which is probably less electronegative than other sp^3 heteroatoms (oxygen and nitrogen) in the compounds, in addition to the sp^2 nitrogen each of them contained. from the results, all of the investigated compounds have the capacity to prevent mild steel corrosion. The molecules adhere to the physical adsorption process, the mechanism, the expected adsorption/binding energies, and the molecule's examined properties all indicate that 2TT is substantially a stronger corrosion inhibitor on Fe(1 1 1), in the following order: 2TT >MDP > 2MI > 2MO.

1. Introduction

Mild steel is known to be an iron metal alloy that is described to be readily available and of low cost [1]. This metal alloy has found great applicability in the design and construction purposes of highly valuable structures and instruments among others [2]. This important metal has been reported in literature to be susceptible to surface corrosion when in contact with alkaline, salts and acid solutions or other aggressive environments. This becomes a serious challenge for the manufacturing industries and other climes that find application of this metal very useful [3-4]. Most highly reactive metals are known to exist as a combined form of an ore which is thermodynamically more stable. Therefore, refined metals are always susceptible to corrosion through oxidation which will return them back to their oxidation states in their stable oxides to attain stability thermodynamically [5]. This process of metal oxidation during corrosion is known to be a spontaneous electrochemical process as reported in literature [6]. Many industrial processes are dependent in using aggressive solutions like acids for oil well acidization, chemical cleaning, pickling, etc [7]. Some of the characteristic metal properties including ductility, conductivity, malleability, hardness, and luster are usually destroyed when the metal is subjected to the aggressive corrosive environments during the oxidative corrosion of the metal. This destruction of some of the physical properties of the metal may result into the failure or reduced efficiency

* Corresponding author.; e-mail: uyerfater22@gmail.com
https://doi.org/10.22034/crl.2023.400989.1226
This work is licensed under Creative Commons license CC-BY 4.0

of the metal's application in construction, machinery and instrumentation purposes [8-9]. For this reason, mild steel metal must be either protected completely or minimize the rate upon which it undergoes corrosion in these aggressive environments. Many methods have been used in literature some of which are highly costly and others which involve the use of synthetic inhibitors are not environmentally friendly [3-5]. Even though the use of inhibitors has found great efficiency in application to curb corrosion, this has tempted corrosion scientists and engineers to find alternative methods of corrosion inhibition using green corrosion inhibitors that are bio-degradable, cheap, effective and easy in application [8]. The phytochemicals serving as green corrosion inhibitors are characterized with presence of heteroatoms such as O, P, S and N and conjugated pi-bonds in their structure [10].

Mechanism of the corrosion inhibition of these compounds proposed in literature explains that these compounds adsorb on the surface of the metal to protect the interaction of the aggressive media with the surface of the metal [11]. Others believe that some of such inhibitors scavenge the ions responsible for the metals corrosion in solution and therefore neutralizes the corrosive effects [1].

Literatures have reported some organic based green inhibitors for the protection of mild steel surface corrosion in acidic medium. The use of 6-bromo-(2, 4-dimethoxyphenyl) methylidene] imidazo [1, 2-a] pyridine-2-carbohydrazide [12], N-substituted carbazoles [13], Chromeno-carbonitriles [14], hydrazinecarboxamides [15], oxadiazole derivatives [16], 2-Pyridinecarboxaldehyde-based Schiff base [17], 3-chloromethylcoumarin derivatives [18], pyridazine derivatives [19] as corrosion inhibitors on mild steel were all studied computationally. In this work, Imidazole, Oxazole, Thiazole and Pyrazole derivatives as nitrogen-based heterocycle compounds were studied theoretically using computational methods of analysis. The high therapeutic properties of the compounds understudy indicate that, it will be available and also economical to use for the corrosion inhibition of metals e.g mild-steel which its Quantum chemical theories were used to determine inhibition potentials of the compounds on mild steel surface. Density functional theory (DFT) methods were used to model the ground state molecular and electronic properties of a system as a function of its electron density distribution [20]. Forcite quench molecular dynamics methods were also used to simulate the molecular interaction of these compounds on Fe (1 1 1) in other to describe the mechanism of the interaction process [21]. These methods were employed to reduce time, error and cost associated with experimental methods of corrosion inhibition studies [9].

The structures of the studied compounds are presented in Fig 1.

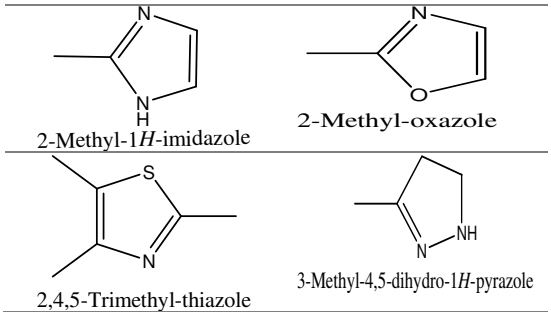

Fig 1: Molecular structure of the studied compounds

2. Materials and methods

2.1. Sketching and Geometric Optimization of the Molecules

ChemDraw Ultra 7.0.3 CambridgeSoft was used to sketch 2D structures of the studied molecules and saved as MDL Molfile (*.mol). Optimization of these molecules with the intention of minimizing the conformational and torsional energies was performed using a DFT method, DMol^3 in BIOVIA Materials Studio Inc software [22-26].

The saved sketched molecules were cleaned upon import into the interactive interphase of the BIOVIA Materials Studio Inc software before geometric optimization. Using DMol^3 package, local density functional was set to B3LYP using DFT-D under restricted spin polarization DNP+ basis which was set in an aqueous medium [23]. During the optimization process some properties of the molecules were set to run along including Fukui indices, total electron density, E_{LUMO} and E_{HOMO} which are examples of Frontier orbitals were all assessed. This is intended to evaluate the sites of local and global reactivity in the molecules [21].

2.2. Quantum Chemical Parameters Calculations

Using the principles of density functional theory (DFT), the quantum chemical parameters of the studied molecules were derived using the DMol3 package of the BIOVIA Material Studio 8.0 software. The B3LYP functional with the "double-numeric plus polarization" (DNP+) basis set in the aqueous phase model was used to calculate the parameters [52-53].

Koopman's theorem was used to evaluate the ionization energy (IP), electron affinity (EA), and other chemical reactivity descriptors that offer insights into chemical reactivity and selectivity in terms of global parameters like electronegativity (χ), hardness (η), and softness (σ), electrophilicity (ω), nucleophilicity (ε) as well as local ones like the Fukui function f(r) [22]. Equations 1-10 were used for such calculations [23]:

IE: Ionization (eV) $IE = -E_{HOMO}$ (1)

AE: Electron affinity (eV) $AE = -E_{LUMO}$ (2)

ΔE_g: Energy gap (eV) $\Delta E_g = E_{LUMO} - E_{HOMO}$ (3)

χ:electronegativity(eV) $\chi = \frac{I+A}{2} = \frac{-1}{2}(E_{HOMO} + E_{LUMO})$ (4)

η: Global hardness (eV) $\eta = \frac{I-A}{2} = -\left(\frac{E_{HOMO} - E_{LUMO}}{2}\right)$ (5)

σ: Global softness $(eV)^{-1}$ $\sigma = -\frac{2}{E_{HOMO} - E_{LUMO}} = 1/\eta$ (6)

ω : Global electrophilicity index (eV $\frac{E_{HOMO} + E_{LUMO}}{8}$ (7)

ε : Nucleophilicity $(eV)^{-1}$ $\varepsilon = \frac{1}{\omega}$ (8)

$\Delta E_{b\text{-}d}$:Energy of back donation(eV) $\Delta E_{b-d}\ \frac{1}{8}(E_{HOMO} - E_{LUMO})$ (9)

ΔN : Fraction of electron(s) transfer $\Delta N = \frac{\chi Fe - \chi Inh.}{2(\eta Fe + \eta Inh)}$ (10)

Where χFe and χinh stand for the absolute electronegativity of iron (Fe) and the inhibitor molecule (inh), respectively, and ηFe and ηinh stand for the absolute hardness of iron (Fe) and the inhibitor molecule. Assuming that for a metallic bulk IP = EA because they are softer than the neutral metallic atoms, values (χFe = 7.0eV) and a global hardness ηFe = 0 and electronegativity of inhibitor (χinh) = 0eV are utilized as a theoretical value for the electronegativity of bulk iron [24]. Another local descriptor is the dual descriptor, or second order Fukui function (f^2). It is described as the difference between electrophilic and nucleophilic Fukui functions. Site k favors a nucleophilic assault if $f^2(r) > 0$, whereas site k prefers an electrophilic attack if $f^2(r) < 0$. This suggests that $f^2(r)$ functions as a selectivity index for nucleophilic or electrophilic assaults. The equations describing the methods of computing the Fukui functions are given in equations (11 – 14) [21]:

Nucleophilic attack $f(k)^+ = qk(N+1) - qk(N)$ (11)

Electrophilic attack $f(k)^- = qk(N) - qk(N-1)$ (12)

Radical attack $f(k)^0 = \frac{qk(N+1) - qk(N-1)}{}$ (13)

Second order function $f(r) = f^+ - f^- = f^2$ (14)

Where qk represents the electron density at a point r in space around the molecule, or the gross charge of atom k in the molecule. The molecule's total number of electrons is denoted by the letter N. An anion is represented by N+1 when a neutral molecule accepts an added electron and N-1 represents a cation with an electron subtracted from the HOMO of the neutral molecule. The ground state geometry served as the basis for all calculations. Using an atomic charge partitioning scheme, such as Mulliken population analysis in equations (11 - 14), these functions were condensed to the nuclei [21].

2.3. Molecular Dynamic Simulations

The molecules of the studied compounds were optimized geometrically using FORCITE tools in the BIOVIA Material Studio 8.0 software. The geometrically optimized molecules were subjected to molecular dynamic simulation on an Fe(1 1 1) surface, with has more densely packed atoms and better stability. The surface of the theoretical iron crystal was subjected to cleaving at a 3.0 Å fractional depth along the (1 1 1) plane.

The surface of the plane was optimized while constraining the bottom layers' geometry and to avoid edge effects, the surface was enlarged into a 4 x 4 supercell. This bigger sizes more than the size of the molecule was chosen to curtail the effect of ghost atoms and as well as edge effects which may affect the results of the molecular dynamic simulations [10]. Each optimized molecule was imported above the cleaved, optimized surface and properly oriented not to pierce the metals surface. To allow the imported molecule which has sufficient kinetic energy to dart around the surface and to prevent the molecule possessing too much kinetic energy that might results in desorption, a 350K temperature was set.

A 5ps simulation time and NVE (microcanonical) ensemble was fixed with a 1fs time step. A 17Å x 12Å x 28Å simulation box was used together with periodic boundary conditions to represent the surface of the metal, COMPASS force field and Smart algorithm were employed for all calculations. Quenching of the system was performed every 250 steps in a total of 5000 cycles resulting into 20 different configurations of the interaction of the molecule with the metals surface. The average adsorption energies of the interaction of each molecule with the metals surface for five different orientations were calculated using equation (15), while the binding energies were calculated using equation (16):

Adsorption Energy = $E_{total} - (E_{inhibitor} + E_{Fe\ surface})$ (15)

Binding Energy = - Adsorption Energy (16)

Where E_{total} is the energy of the molecule/metal complex, $E_{inhibitor}$ is the energy of the molecule only and $E_{Fe\ surface}$ is the energy of the iron surface respectively [17,23-26, 30, 40-48].

3. Results and Discussion

During geometric optimization of the studied compounds using $DMol^3$ package in the BIOVIA Materials studio software, some properties were selected which include total electron density, molecular orbitals of HOMO and LUMO and the results in terms of snap shots of the plotting were reported in Fig 2.

In order to establish the local reactivity of the studied molecules, Fig 3 presents the molecular structure of the labelled atoms to allow for easy identification of the local points of attack in the molecules.

Table 2 contains the summary of the Hirshfield values of the nucleophilic point of attack (f^+) and as well as that of the electrophilic point of attacks (f^-) in the studied molecules. Fig 4 are individual molecular graphical representation of the second order Fukui functions of the molecules which describes the global reactivity of the molecules, whether they are entirely nucleophilic or electrophilic in nature. The percentage of second Fukui function showing electrophilic and nucleophilic values of the studied molecules are presented in Table 3 for comparison.

After the Forcite quench molecular dynamic simulations, the lowest energy orientation of the simulated products was selected. Fig 5 presents the snap shots of each simulated molecule on top and side view on the Fe(1 1 1) surface. In order to establish whether there was adsorption of the molecules on the surface of the Fe(1 1 1) surface, the molecular bond lengths and angles before and after adsorption were measured and compared.

Table 4 presents the bond length of the molecules before and after simulation, while Table 5 contains the bond angle of the studied molecules before and after simulation. To be able to appraise the nature of the interaction of the molecules on the surface of Fe(1 1 1) quantitatively, adsorption and binding energies of the interaction were calculated and presented in Table 6. Results of all the derived Frontier energies and the calculated quantum chemical parameters of the studied molecules which describes the electronic distribution and charge transfer are as presented in Table 1.

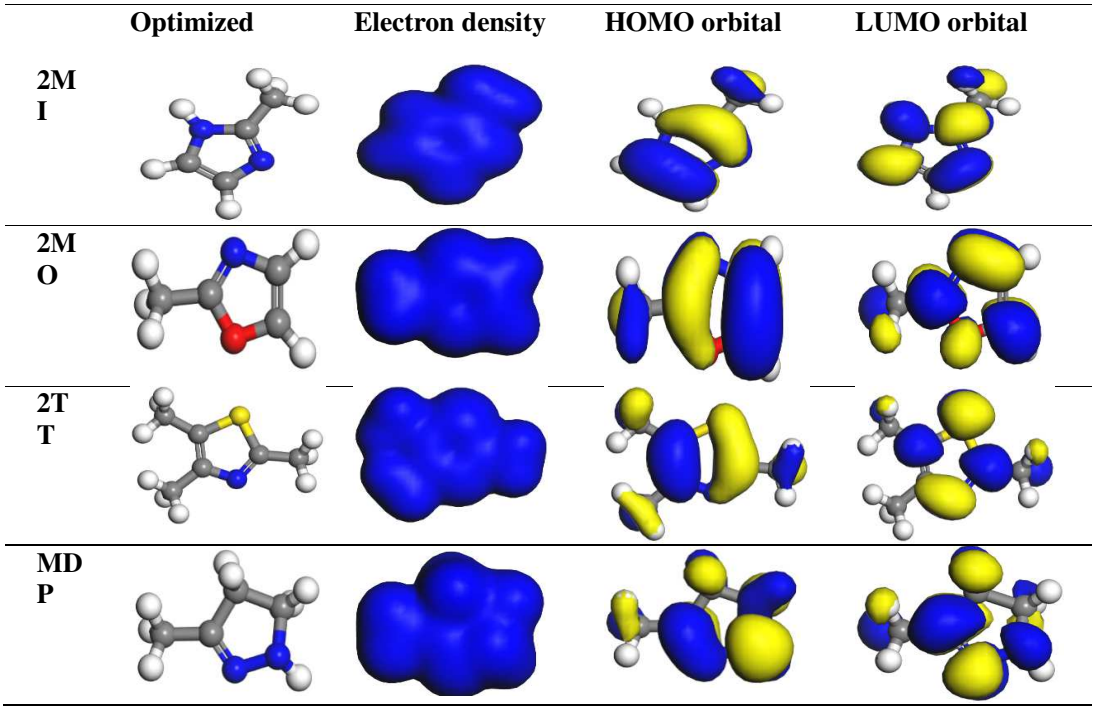

Fig 2: Optimized structure, electron density, HOMO and LUMO orbitals of the studied molecules

Table 1: The Frontier Energies of the research molecules.

Parameters	2MI	2MO	2TT	MDP
E_{HOMO} (eV)	-5.885	-5.748	-5.407	-4.641
E_{LUMO} (eV)	-1.007	-0.746	-1.353	-0.507
ΔE_g (eV)	4.878	5.002	4.054	4.134
μ (Debye)	3.610	1.370	0.110	1.800
IE = $-E_{HOMO}$ (eV)	5.885	5.748	5.407	4.641
AE = $-E_{LUMO}$ (eV)	1.007	0.746	1.353	0.507
χ (eV)	3.446	3.246	3.380	2.574
η(eV)	2.439	2.501	2.027	2.067
σ $(eV)^{-1}$	0.410	0.400	0.493	0.484
ω (eV)	2.434	2.106	2.818	1.603
ε $(eV)^{-1}$	0.411	0.475	0.355	0.624

$\Delta E_{b\text{-}d}$ (eV)	-0.610	-0.625	-0.507	-0.517
ΔN	0.729	0.750	0.893	1.071

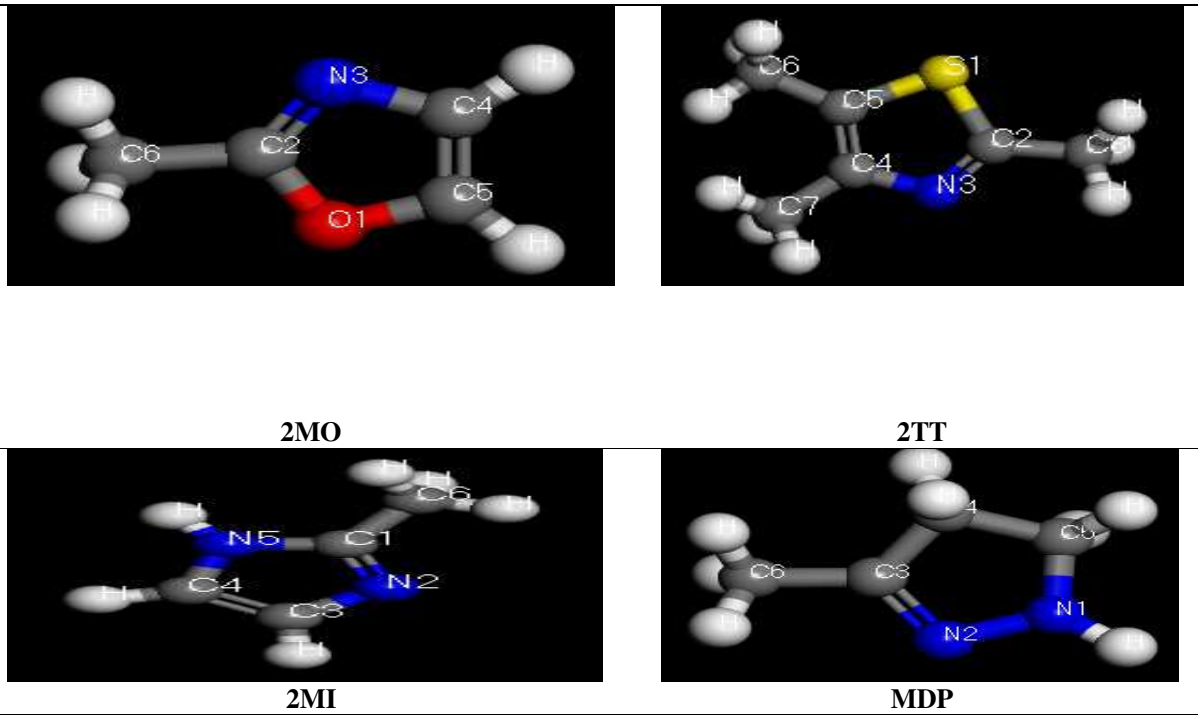

Fig 3: Labelled atoms of the studied molecules

Table 2: Calculated Fukui functions of the molecules

Inhibitor	Atom	Nucleophilic Attack (+) Hirshfield	Electrophilic Attack (-) Hirshfield
2MI	C(4)	0.145	0.198
2MO	C(5)	0.153	0.207
2TT	S(1)	0.245	0.162
MDP	N(2)	0.237	0.111

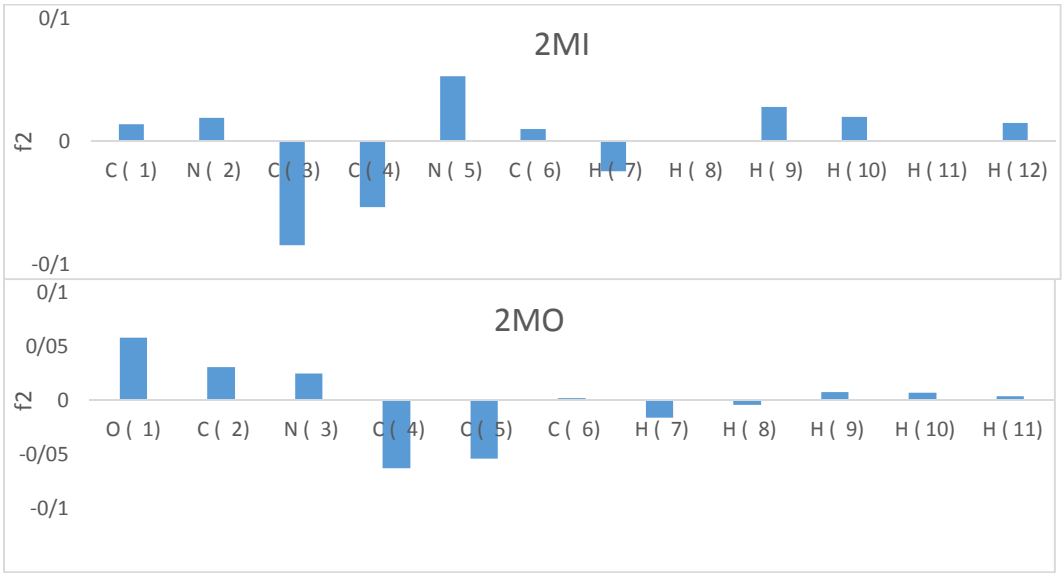

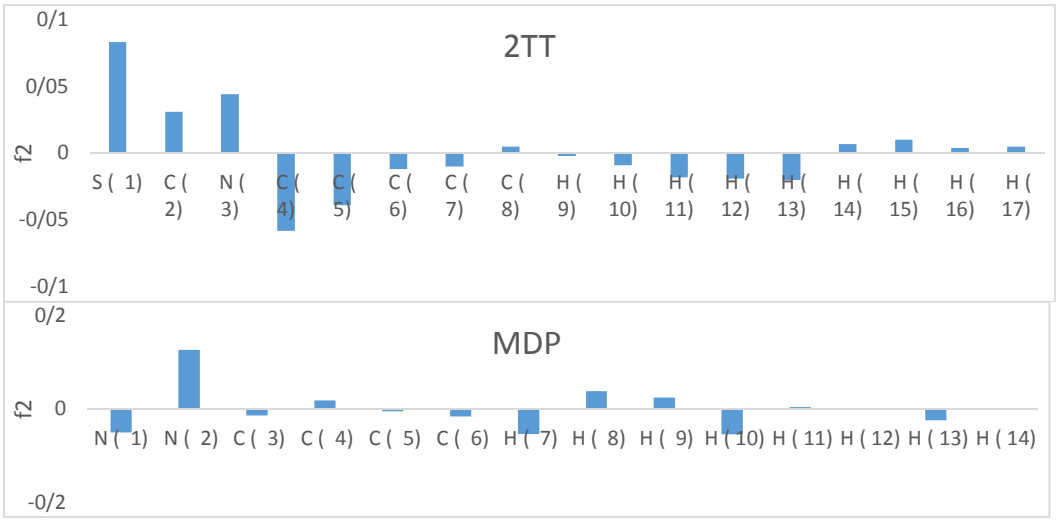

Fig 4: Graphical representation of the second Fukui function

Table 3: Percentage of second Fukui function showing electrophilic and nucleophilic values

Molecule	f^{2+}(%)	f^{2-}(%)
2MI	57.1	42.9
2MO	54.5	45.5
2TT	66.7	33.3
MDP	50.0	50.0

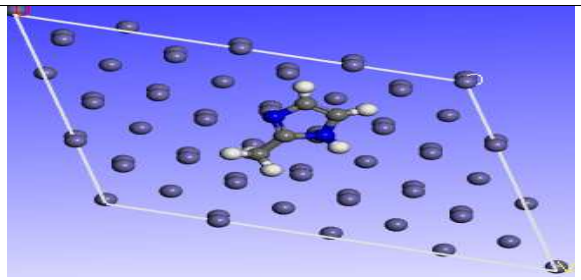

On top view of 2MI on the surface

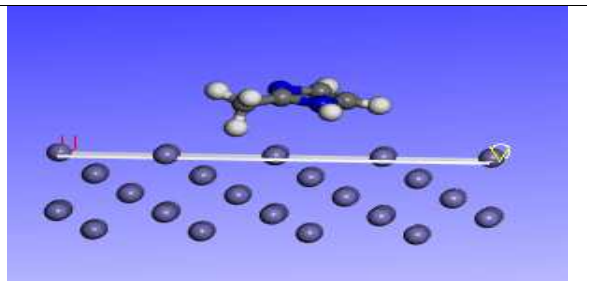

Side view of 2MI on the surface

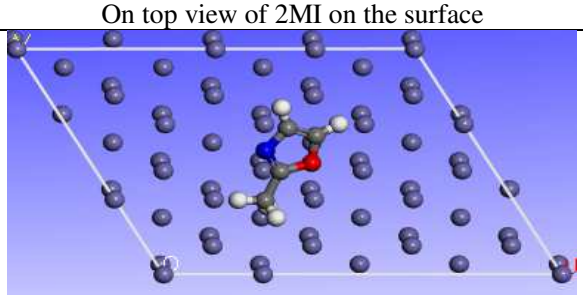

On top view of 2MO on the surface

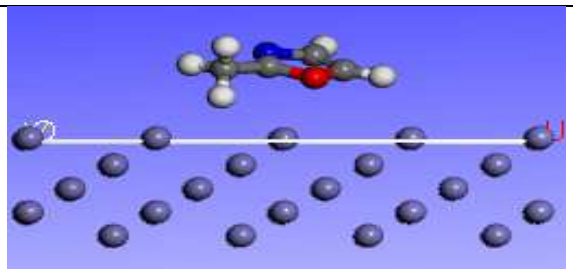

Side view of 2MO on the surface

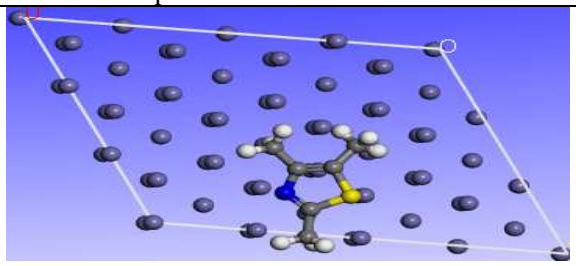

On top view of 2TT on the surface

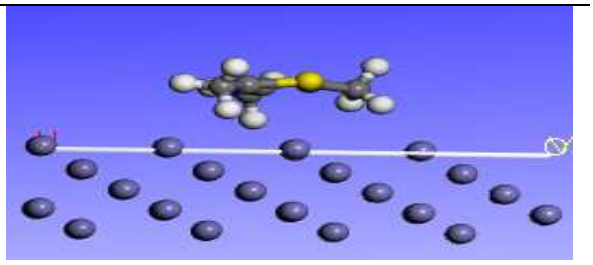

Side view of 2TT on the surface

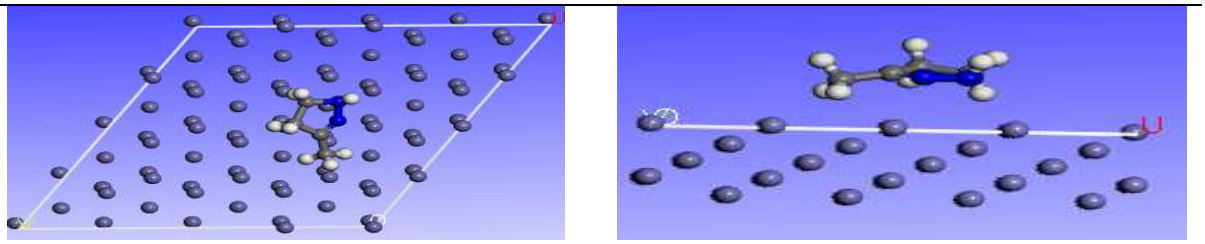

On top view of MDP on the surface | Side view of MDP on the surface

Fig 5: Simulated molecule on top and side view on the Fe (111) surface

Table 4: Bond length of the molecules before and after Simulation

Molecule	Bond length type	Before adsorption (Å)	After adsorption (Å)	Difference (Å)
2MI	C1-N2	1.332	1.332	0.000
	N2-C3	1.359	1.357	0.002
	C3-C4	1.370	1.370	0.000
	C4-N5	1.372	1.371	0.001
	N5-C1	1.383	1.382	0.001
	C1-C6	1.498	1.499	0.001
2MO	O1-C2	1.382	1.382	0.000
	C2-N3	1.317	1.317	0.000
	N3-C4	1.370	1.359	0.011
	C4-C5	1.360	1.363	0.003
	C5-O1	1.361	1.363	0.002
	C2-C6	1.499	1.497	0.002
2TT	S1-C2	1.716	1.715	0.001
	C2-N3	1.312	1.312	0.000
	N3-C4	1.378	1.380	0.002
	C4-C5	1.391	1.390	0.001
	C5-S1	1.711	1.710	0.001
	C5-C6	1.493	1.493	0.000
	C4-C7	1.497	1.497	0.000
	C2-C8	1.499	1.480	0.019
MDP	N1-N2	1.319	1.318	0.001
	N2-C3	1.254	1.254	0.000
	C3-C4	1.492	1.490	0.002
	C4-C5	1.608	1.608	0.000
	C5-N1	1.499	1.495	0.004
	C3-C6	1.507	1.503	0.004

Table 5: Bond angle of the studied molecules before and after Simulation

Molecule	Bond angle type	Before adsorption (^{0})	After adsorption (^{0})	Difference (^{0})
2MI	C1-N2-C3	106.935	107.029	0.094
	N2-C3-C4	110.702	110.645	0.057
	C3-C4-C5	105.180	105.191	0.011
	C4-N5-C1	108.177	108.235	0.058
	N5-C1-C6	124.689	124.918	0.229
	C6-C1-N2	126.308	126.107	0.201
2MO	O1-C2-N3	111.119	111.066	0.053
	C2-N3-C4	106.223	106.321	0.098
	N3-C4-C5	109.274	109.202	0.072
	C4-C5-O1	107.669	107.730	0.061
	O1-C2-C6	123.994	124.160	0.166
	C6-C2-N3	124.887	124.703	0.184
2TT	S1-C2-N3	113.789	113.891	0.102
	C2-N3-C4	111.971	111.970	0.001
	N3-C4-C5	114.222	114.210	0.012
	C4-C5-S1	109.230	109.111	0.119
	C6-C5-S1	118.563	116.510	2.053
	N3-C4-C7	121.300	120.311	0.989
	S1-C2-C8	118.334	118.111	0.223

MDP	N1-N2-C3	139.457	139.997	0.540
	N2-C3-C4	98.790	98.342	0.448
	C3-C4-C5	100.372	100.546	0.174
	C4-C5-N1	110.929	110.976	0.047
	N2-C3-C6	124.875	124.025	0.850

Table 6. Calculated molecular dynamic simulation parameters for the studied molecules

Properties (kcal/mol)	2MI	2MO	2TT	MDP
Total kinetic energy	6.74±1.1	4.95±1.6	11.15±5.73	7.93±0.2
Total potential energy	-50.49±1.5	-32.55±2.7	-53.79±9.8	-4.94±4.2
Energy of the molecule	-9.09±0.0	5.66±0.0	2.69±2.7	3.90±0.2
Energy of the surface	0.00±0.0	0.00±0.0	0.00±0.0	0.000±0.0
Adsorption energy	-41.40±0.0	-38.21±0.0	-56.48±0.6	-44.32±0.2
Binding energy	41.40±0.0	38.21±0.0	56.48±0.6	44.32±0.2

4. Discussion

4.1Frontier molecular orbitals

Due to statistical calculations' accuracy and lack of human error, quantum chemical calculations are increasingly being used in corrosion investigations [25]. This work examined the inhibitors' selectivity and suggested a possible interaction between the molecules of the inhibitors and the metal surface [26]. This inhibition reactivity is determined by the inhibitor's electronic characteristics, such as the presence of pi-bonds (partial charges on the molecules), electron density, etc., which are influenced by the existence of the kind of functional groups in the inhibitor's molecule [27]. As local and global reactivity of the interaction are calculated from the derived HOMO and LUMO eigen values data, the nature of the LUMO, HOMO and total electron density overlap also have an impact on the effect of the interaction of the molecules on the metal surface. The HOMO area denotes the locations of nucleophilic assault, whereas the LUMO orbital denotes the location of electrophilic attack on the molecule [28-30]. Depending on how the molecules interact with the metal surface, the molecule can either donate electron(s) to the mild steel's empty d-orbital (nucleophilic) or accept electron(s) from the metal surface to an electrophilic region of itself [31-32]. In Fig 2, the colors represent the distinction between the atoms in the molecules with white H, gray C, blue N, yellow S and red O. The molecules are referred to by their abbreviations, which are MDP for 3-methyl-4,5-dihydro-1H-pyrole, 2MI for 2-methyl-1H-imidazole, 2MO for 2-methyl-oxazole and 2TT for 2,4,5-trimethyl-thizole.

The discovery of electron has tremendously helped in describing the behavior of molecular entities in which the electronic distribution of a molecule's molecular orbitals determines how chemically reactive it is, demonstrating that an atom is not a vacuous substance. From Fig 2, it can be observed that the entire structure of the four compounds studied were covered completely with their electron density which suggests that most parts of the molecule will have contact with the metals surface and be able to enhance adsorption on the metal surface. The HOMO orbitals of 2MI are found to be located around the nitrogen heteroatoms of the molecule, while that of 2MO around nitrogen and oxygen atoms of the heterocycle. For 2TT the HOMO orbitals overlap around the sulphur-nitrogen heteroatom moieties, while that of MDP was around the α-nitrogen heteroatoms. The location of the LUMO orbitals were found to vary from one molecule to another. This is an indication that the molecules can serve as promising inhibitors because of their electron donating activity as reflected by their HOMO orbitals all situated around the electron rich heteroatoms of the studied molecules [33].

4.2. Frontier orbital energies and associated parameters

In this study, the Frontier orbital energies calculated were E_{HOMO}, E_{LUMO}, energy gap (ΔE_g), dipole moment (μ), and the associated parameters include: absolute electronegativity (χ), global hardness (η), global softness (σ), global electrophilicity index (ω), nucleophilicity (ε), energy of back donation ($\Delta E_{b\text{-}d}$) and proportion of electron(s) transfer (ΔN) from the molecule to the metal atoms. The highest occupied molecular orbital energy of each moiety, or the E_{HOMO} value, indicates the possibility for electron donation from the molecule to the open d-orbitals of the metal surface (mild steel). On the other hand, E_{LUMO}, which stands for lowest unoccupied molecular orbital, is connected to the acceptance of electrons from the metal surface by the studied molecule. Table 1 presented the list of the calculated and derived energies. The Frontier molecule results from Table 1 suggest that the molecules will be able to adsorb and

donate electrons to the surface of mild steel (Fe) [34]. According to the findings, molecules' E_{HOMO} values are in the following order: MDP > 2TT > 2MO > 2MI, whereas their E_{LUMO} values did not follow any appreciable order of pattern. Therefore, a high E_{HOMO} value indicates a strong nucleophilic (high donation power) character of the molecule and its tendency to donate electrons to low empty orbital energy, but a low E_{LUMO} value indicates an electrophilic nature, which increases the likelihood of the molecule accepting an electron [35]. The extent of the interaction of the inhibitor molecule with the surface of the metal increases with a lower E_{LUMO} and a higher E_{HOMO} values. The E_{LUMO} values here reported are in divergent with the trend of E_{HOMO} reported. With this MDP is the most likely a better inhibitor in relation to other molecules studied.

The energy gap ΔE_g of the frontier orbitals energies is an important parameter that demonstrates the reactivity of a molecule in relation to the metals surface. This is the gap in energy between reacting substances, allowing for efficient electron transmission between them [36]. Energy gap values that are large are known to be related to low reactivity in molecules because the energy involve moving electrons from E_{LUMO} to E_{HOMO} is very large for such chemical species [37]. While lower energy gap values are known to improve the reactivity of substances possessing them because of the ease to move electrons from their E_{LUMO} to their E_{HOMO} [38]. The energy gap parameter can be used to describe the stability of a molecule adsorbed to the surface of a metal as its value decreases the inhibition efficiency is expected to subsequently increase [39]. The trend observed for the studied compounds is as follows: 2MO> 2MI> MDP> 2TT with 2TT having the lowest value and more reactive and most stable.

The polarity as shown by the dipole moment is one of the important parameters that describe a molecule electronically interms of the non-uniform distribution of atoms charges [23]. Also reactivity is the capacity to lose or gain electron(s), which is determined by the separation of electric charge within a molecule, which depends on the electronegativity of the molecules [29]. High values of the dipole moment may in one way increase the extent of the interaction between the metal surface and the studied molecule. This is as a result that the deformation energy which increases with increase in dipole moment resulting in easy interaction of a given molecule with the surface of the metal. This may eventually increase the corrosion inhibition of the molecule on the metals surface. From Table 1, the order of the derived dipole moment is given by 2MI>MDP>2MO> 2TT, with 2TT having the least polarity while 2MI has the highest. This trend did not conform with any of the two earlier parameters discussed.

The absolute electronegativity (χ) is in the same order as the molecular E_{LUMO}, indicating that the molecular reactivity values are consistent with the molecular ionization energy [30]. The ability of the molecules to draw electrons to themselves is demonstrated by their electron affinity. Molecules that possess low electronegativity difference with high electronegativity, values according to the electronegativity equalization principle of Sanderson, are known to easy equalization which in turn results in low reactivity and resultant lower corrosion inhibition potentials [40]. Among the tested compounds reported in Table 1, 2MI should have the highest electron affinity and therefore less reactive when compared to MDP.

On the other hand, the molecules' overall softness (σ) balances out their overall hardness (η). As both softness and hardness are descriptors of global chemical behavior which measures the reactivity and stability of molecules [39]. The polarization or deformation resistance of atom, molecule or ions electron cloud towards small perturbations in chemical reaction is apparently known as chemical hardness [39]. While the other way round describes the molecules global softness. Therefore, large energy gap is associated to a hard molecule, while small energy gap describes a soft molecule [23]. The molecule who has relatively low global hardness and high global softness will potentially be a better corrosion inhibitor because electrons are easily transferred during adsorption of the molecule on the metals surface. From the results presented in Table 1, 2TT have relatively the lowest global hardness and the highest global softness and therefore more likely to be a better inhibitor in this regard which is in good agreement with results earlier reported for energy band gap.

An important entity which also describe the nature of the interaction between the metals surface and the inhibitor molecule is the energy of back donation $\Delta E_{b\text{-}d}$. Gomez et al. [41] was first to propose this important parameter. It was reported by Bedair [42] that if the energy of back donation is found to be negative and the global hardness value is positive, the back donation of electrons to the molecule is an energetically favorable process. An inverse relationship is established between the global hardness and energy of back donation, as the earlier decreases the later increases. Since all the studied molecules are interacting with the same metals surface, the stabilization that may result for the inhibitor compounds can be compared. From Table 1 all the values of the back-donation energies are negative, while their global hardness values are positive. This is an indication that they all favor the back donation of electron process favorably. Relatively 2TT (2TT>MDP>2MI> 2MO) has the highest energy of

back donation and therefore is more energetically favored when compared to others.

Another molecular reactivity index is the fraction of electron(s) transfer (ΔN) from the molecule to the metal atoms. This measures the relative energy stabilization when the system acquires electronic charges and this qualifies the effectiveness of the inhibition process. According to Lukovit's study [43], increasing inhibition efficiency is experienced with the molecules electron donating ability to the metals surface if the fraction of electron(s) transfer is less than 3.6 value and vice versa. Table 1 presents the following order in the values of ΔN: MDP>2TT>2MO>2MI with all their values less than 3.6. This is an indication that the inhibition efficiency of the studied compounds may not increase with an increase in electron donating abilities to the metals surface atoms.

Parr et al. [44] introduced the global electrophilicity index (ω) which is a measure of energy lowering due to maximal flow of electrons the acceptor and donor entities. With this the propensities of molecules to accept electrons can simply be measured by this parameter. The inverse of the electrophilicity index is the nucleophilicity (ε) which describes the ability of chemical specie to share electrons [23]. Lower values of electrophilicity index is characterized by a reactive nucleophile, while high values describe an electrophilic chemical specie. Electrophilicity index with large values for molecules are indicators of poor corrosion inhibition, while those with high nucleophilicity values happens to be excellent corrosion inhibitors [45]. Large values of electrophilicity index was reported in Table 1 for the molecules which is due to the high reliance of B3LYP functional on electronegativity with 2TT relatively having the highest and a better nucleophile than others.

4.3. Fukui function

With the aid of Fukui of various functions, the studied compounds local reactivities were investigated. The Fukui indices are known to indicate the areas that are more reactive to radical, electrophilic, and nucleophilic assaults. However, the focus of this work was on nucleophilic and electrophilic points of attack on the molecules under review. The Fukui operates electrophilic (f^-) and nucleophilic (f^+) reactions sites and assesses the orbital areas of selectivity [10]. These demonstrate the significance of examining the mechanisms behind the inhibitors' interactions with surfaces. The atom in the molecule with the highest Hirshfield or Milliken value, which indicates the region where reaction is likely to occur in the molecule, is where these nucleophilic and electrophilic attacks are observed. Only Hirshfield was taken into account in this investigation because they displayed relatively higher values. The atoms with highest eigen values obtained from Hirshfield evaluations of the molecules are shown in Table 2. In the 2MI moiety, the C(4) atom has the highest calculated Fukui functions in both the nucleophilic attack (+) and the electrophilic attack (-), indicating that C(4) is the molecule in which the majority of reactions may take place. The 2MO has its highest region of reactivity at the C(5) atom for both the nucleophilic attack (+) and the electrophilic attack (-), while the 2TT is on the S(1) atom for both the nucleophilic attack (+). The highest values for MDP are found on N(2) atom of the molecule. These regions of reactivity may be linked to the molecule's heteroatom and pi-bond moieties. Molecules could have their highest Eigen values for nucleophilic and electrophilic attack on the same atom indicating such atom with the highest reactivity in the molecule [46]. Therefore, it could be seen that the heteroatoms namely: nitrogen, oxygen and sulphur in the studied molecules could be responsible for the nucleophilic and electrophilic attacks on the surface of Fe in the corrosion inhibition process of the metal (Fig 3).

The second order Fukui function (f^2) is a global reactivity parameter which try to distinguish the nucleophilic or electrophilic nature of the molecule as an entity. Fig 4 and Table 3 are the presentation of the calculated values as well as the graphical representation of the distribution of the Fukui indices with respect to each atom of the molecule. It can be observed from the table and Figs that the values of $f^2 > 0$ (positive second order Fukui functions) of the studied molecules are: 2TT (66.7%), 2MI (57.1%), 2MO (54.5%) and MDP (50.0%) respectively. Values for the negative second order Fukui functions ($f^2 < 0$) for the studied molecules are: 2TT (33.3%), 2MI (42.9%), 2MO (45.5%) and MDP (50.0%) respectively. Based on these values, it can be inferred that 2TT is relatively more nucleophilic than others with respect to the inhibition of the corrosion of iron metals surface. Herein, the order for the inhibition efficiency with respect to the nucleophilicity of the molecules is 2TT>2MI>2MO>MDP.

4.4. Molecular Dynamic Simulations

To provide additional information on the understanding of the studied compounds corrosion inhibition potentials on iron metals surface, simulation of the molecules and the surface was conducted [47]. This is aimed at studying the interaction of each molecule with the iron metals surface to generate data that can be used to predict the inhibition efficiencies of the molecules. FORCITE quenching method of molecular dynamic simulation was used to model the corrosion inhibition process as contained in BIOVIA Material Studio 8.0. Smart algorithm with a periodic

boundary in a simulation box of 17Å x 12 Å x 28 Å was used and COMPASS force field was used for the calculations [48]. The on top and side view snap shots of the lowest energy interaction between each molecule and the Fe(1 1 1) surface during the simulation are as presented in Fig 5. It can be observed that each molecule has a flat lying orientation on the Fe(1 1 1) surface with almost all their atoms in contact with the Fe(1 1 1) surface atoms. This may be due to the structural and electronic distribution nature of these molecules which are made of a 5-membered ring heterocycle with relatively few substituents to allow structural deformity during geometric optimization and dynamic simulations. The interaction of the studied molecules with the surface of the Fe(1 1 1) metal may result in changes of the bond length in each molecule during simulation. For such a reason, the bond lengths of the molecule after optimization before docking on the surface of the metal were measured and compared to the lowest energy configuration bond lengths of the molecule after molecular dynamic simulation. The addresses of the bond lengths between the atoms can be referred to in Fig 3 which contained the labelled atoms of each molecule. The results of the bond length measurements before and after simulations are as presented in Table 4 for comparison. Bond lengths in 2MI did not show any significant difference before and after simulation. For 2MO also most of the bond lengths did not change reasonably in dimension during simulation with exception of N3-C4 bond that had a difference of 0.001Å in length. Similar results obtained for 2MO was also noticed for 2TT with the only variation in bond length of C2-C8 that also decreased by 0.019Å in length. MDP molecule did not show any significant change in bond length as a result of the quenched molecular dynamic simulation. It is anticipated that with the rigid cyclic nature of the studied molecules that possess few side chains, bond lengths in these molecules may not be significantly be distorted as a result of the molecular dynamic simulations [24, 49-50]. To further qualify the nature of the adsorption of the studied molecules on the surface of Fe(1 1 1) metal, the bond angles of the geometrically optimized molecule was measured and compared with that of the adsorbed molecule after dynamic simulation. The bond regions filled by the heteroatoms were given more attention while calculating the molecules' bond angle. The addresses of the bonds are as given in Fig 3, while the results of the bond angle measurements are reported in Table 5. According to the measured bond angles, all inhibitor molecules studied have bond angles that are between 90^o and 230^o respectively. Even though the nature of the hybridization of atoms in these compounds ranged from sp^2 and sp^3 with n and π – electron atoms, the overall geometries of the molecules cannot be described by a single type of geometry [24, 49-50]. As reported in Table 5, all the studied molecules reported variation significantly in some of the bond angles measured. For 2MI: N5-C1-C6 and C6-C1-N2, 2MO: O1-C2-C6 and C6-C2-N3, 2TT: C4-C5-S1, C6-C5-S1, N3-C4-C7 and S1-C2-C8, MDP: N1-N2-C3, N2-C3-C4, C3-C4-C5 and N2-C3-C6 respectively. Values of variation in 2TT were more significantly different before and after adsorption during the molecular dynamic simulation.

To quantify the extent of the interaction of each molecule on the surface of Fe (1 1 1) during the quenched molecular dynamic simulation, both adsorption and binding energies of the interaction were computed and reported in Table 6. All adsorption energies were reported to be negative and relatively low; this proves the adsorption process. Because both the calculated adsorption and binding energy values are below the thresholds for chemisorption, which are respectively -100kcal/mol and 100kcal/mol, the mechanism of the molecules adsorption on the surface of Fe(1 1 1) is physisorption [51]. The trend in the adsorption/binding energies of the molecules is as follows: 2TT>MDP>2MI>2MO. Literature have indicated that the more negative the adsorption energy or the more positive the binding energy the better the inhibition process [51]. From Table 6, the relatively highest value is obtained for 2TT and therefore demonstrated that 2TT is more efficient and effective in adsorbing on the surface of Fe(1 1 1) and therefore a better inhibitor [23]. According to the literature, molecules having the S- heteroatom are more effective at adhering to mainly FCC metals of which iron is an example [52]. When the four heterocycles are compared, it can be observed that they all have an sp^2 nitrogen common to them, but in addition 2MI has another sp^3 nitrogen at a 1,3 position to the sp^2 nitrogen, 2MO has and additional sp^3 oxygen at 1,3 position with the sp^2 nitrogen, 2TT has an sp^3 sulphur at a 1,3 position to the sp^2 nitrogen and MDP has an sp^3 nitrogen at a 1,2 position to the sp^2 nitrogen. When the sizes of these three heteroatoms (N, S and O) are compared, relatively S should be less electronegative and more willing to donate its lone pair of electrons during interaction. This is the reason why its adsorption/binding energies are relatively higher than the remaining and therefore a better corrosion inhibitor on Fe(1 1 1) surface.

5. Conclusion

Mild steel is one of the most important metals on earth and is known to be severely affected by deleterious effects of corrosion. For such a reason, it therefore needs to be protected. Many methods of corrosion are employable but the use of organic-green corrosion inhibitors is the most preferable. This work tried to

establish the corrosion inhibition efficiency of some selected nitrogen-based heterocycle compounds on mild steel and to propose a possible mechanism for the inhibition process theoretically. Quantum chemical calculations of the geometrically optimized molecules and quench molecular dynamic simulation of the inhibition process was conducted. The results of this study demonstrated the efficacy of 2,4,5-trimethyl-thizole (2TT), 3-methyl-4,5-dihydro-1H-pyrole (MDP), 2-methyl-oxazole (2MO) and 2-methyl-1H-imidazole (2MI) as corrosion inhibitors on the surface of iron metal through adsorption processes. The presence of several hetero atoms rich in n-electrons, pi-bonds, molecular geometry and charge distribution among other factors, are observed to be responsible for the corrosion inhibition potentials of the studied molecules. The results showed that the adsorption or binding energy of each molecule on the Fe(1 1 1) surface is negative and relatively low, less than +100kcal/mol threshold which signifies all of them to obey the mechanism of physical adsorption. However, it has also been found that in total aggregates of the parameters studied, 2TT molecule is potentially more effective in the corrosion inhibition of Fe(1 1 1) surface. This is because of the presence of a sp^3 sulphur heteroatom in its structure that is less electronegative than the sp^3 oxygen, sp^3 nitrogen and sp^2 nitrogen atoms in the other compounds in addition to the sp^2 nitrogen each of them possessed.

LIST OF ABBREVIATIONS

2MI: 2-methyl-1H-imidazole; 2MO: 2-methyl-oxazole; 2TT: 2,4,5-trimethyl-thizole; MPP: 3-methyl-4,5-dihydro-1H-pyrole (MPP); DFT: Density functional theory; B3LYP: Becke 3-parameter Lee-Yang-Parr; DNP: Double numerical polarization; COMPASS: Condensed-phase optimized molecular potentials for atomic simulation studies; E_{HOMO}: Energy of the highest occupied molecular orbital; E_{LUMO}: Energy of the lowest unoccupied molecular orbital.

DECLARATIONS

Ethics approval and consent to participate

Not applicable.

Consent for publication

Not applicable.

Competing interests

The authors declare that they have no competing of interests.

Funding

No funding was obtained for this study.

Authors' Contributions

FI did the conception, designed the work and conducted the computational work; ASM and NTA interpreted the data; AMA developed and revised the manuscript. All authors read and approved the final form of the manuscript.

ACKNOWLEDGEMENTS

The installation of the BIOVIA Material Studio 8.0 software was done with assistance from Dr. David Ebuka Arthur of the Department of Pure and Applied Chemistry, University of Maiduguri, Borno State, Nigeria, which the authors gratefully welcome.

References

[1] K. Akbarzade, Danaee I., Nyquist plots prediction using neural networks in corrosion inhibition of steel by schiff base, *Iranian Journal of Chemistry and Chemical Engineering (IJCCE),* 37(3):135-43 (2018).

[2] B.N Noorollahy, Hafizi-Atabak HR., Atabaki F., Radvar M., Jahangiri S., Electrochemical Measurements for the Corrosion Inhibition of Mild steel in 0.5 M HCl Using poly (epichlorohydrin) Derivatives, *Iranian Journal of Chemistry and Chemical Engineering (IJCCE),* 39(4):113-25 (2020).

[3] [3] Afandiyeva L., Abbasov V., Aliyeva L., Ahmadbayova S., Azizbeyli E., El-Lateef Ahmed HM., Investigation of Organic Complexes of Imidazolines Based on Synthetic Oxy-and Petroleum Acids as Corrosion Inhibitors, *Iranian Journal of Chemistry and Chemical Engineering (IJCCE),* 37(3):73-9 (2018).

[4] V. Grudic V., Boskovic I., Radonjic D., Jacimovic Z., Knezevic B., The electrochemical behavior of Al alloys in NaCl solution in the presence of pyrazole derivative, *Iranian Journal of Chemistry and Chemical Engineering (IJCCE)*, 38(2):127-38 (2019).

[5] E.M Robert EM., Wells T., Corrosion between soil electrical resistance and corrosion of steel, *International journal of corrosion processes and corrosion control*, 53(7) (2018). Doi.org/10.1080/1478422X.2008.1511325.

[6] T.F Maryer, Gehlen C., Deuberschmidt C., Corrosion monitoring in concrete, Woodhead publishing series: In metals and surface engineering, 379-405 (2021). Doi.org/10.10161b978-0-08-103003-5-00016-3.

[7] S. Jyothi, Rathidevi K., Experimental and theoretical investigation on corrosion inhibition of mild steel in sulphuric acid by coccinia indica leaves extract, *R. J. Chem.* 10(4): 1253-1260 (2017).

[8] L.T Popoola LT., Aderibigbe TA., Lala MA., Mild Steel Corrosion Inhibition in Hydrochloric Acid Using Cocoa Pod Husk-Ficus exasperata: Extract Preparation Optimization and Characterization, *Iranian Journal of Chemistry and Chemical Engineering (IJCCE)*, 41(2):482-92 (2022).

[9] H. Lgaz, Salghi R., Chaouiki A., Shubhalaxmi S., Jodeh K., Bhat S., Pyrazoline derivatives as possible corrosion inhibitors for mild steel in acidic media: A combined experimental and computational approach, *Cogent Engineering* 5: 1441585 (2018).

[10] N.O Eddy, Ameh PO., Essien NB., Experimental and computational chemistry studies on the inhibition, *Taibah University Journal for science*, 12(5): 545-556 (2018).

[11] P. Shwethambika, Ishwara Bhat J., Matured Theobroma Cocoa Pod Extracts as Green Inhibitor for Acid Corrosion

of Aluminium, *Iranian Journal of Chemistry and Chemical Engineering (IJCCE),* 40(3):906-19 (2021).

[12] K.V Shenoy KV., Venugopal PP., Kumari PR., Chakraborty D., Effective inhibition of mild steel corrosion by 6-bromo-(2, 4-dimethoxyphenyl) methylidene] imidazo [1, 2-a] pyridine-2-carbohydrazide in 0.5 M HCl: Insights from experimental and computational study, *Journal of Molecular Structure*, 1232: 130074 (2021).

[13] H.U Nwankwo, Akpan ED., Olasunkanmi LO.., Verma C, Al-Mohaimeed AM., Al Farraj DA., Ebenso EE., N-substituted carbazoles as corrosion inhibitors in microbiologically influenced and acidic corrosion of mild steel: Gravimetric, electrochemical, surface and computational studies, *Journal of Molecular Structure*, 1223: 129328 (2021).

[14] T,W Quadri TW., Olasunkanmi LO., Akpan ED., Alfantazi A., Obot IB., Verma C., Quraishi MA., Chromeno-carbonitriles as corrosion inhibitors for mild steel in acidic solution: electrochemical, surface and computational studies, *RSC advances*, 11(4): 2462-2475 (2021).

[15] L.O Olasunkanmi LO., Aniki NI., Adekunle AS., Durosinmi LM., Durodola SS., Wahab OO., Ebenso EE., Investigating the synergism of some hydrazinecarboxamides and iodide ions as corrosion inhibitor formulations for mild steel in hydrochloric Acid: Experimental and computational studies, *Journal of Molecular Liquids*, 343: 117600 (2021).

[16] V. Kalia V., Kumar P., Kumar S., Goyal M., Pahuja P., Jhaa G., Verma C., Synthesis, characterization and corrosion inhibition potential of oxadiazole derivatives for mild steel in 1M HCl: Electrochemical and computational studies, *Journal of Molecular Liquids*, 348: 118021 (2022).

[17] X.L Li, Xie B., Feng JS., Lai C., Bai XX., Li T., Gu YT., 2-Pyridinecarboxaldehyde-based Schiff base as an effective corrosion inhibitor for mild steel in HCl medium: Experimental and computational studies, *Journal of Molecular Liquids*, 345: 117032 (2022).

[18] T.O Olomola, Durodola SS., Olasunkanmi LO., Adekunle AS., Effect of selected 3-chloromethylcoumarin derivatives on mild steel corrosion in acidic medium: experimental and computational studies, *Journal of Adhesion Science and Technology*, 1-15 (2022).

[19] [R.O Ogede RO., Abdulrahman NA., Apata DA., DFT computational study of pyridazine derivatives as corrosion inhibitors for mild steel in acidic media, *GSC Advanced Research and Reviews*, 11(3): 106-114 (2022).

[20] H. Jafari H., Mohsenifar F., Sayin K., Effect of alkyl chain length on adsorption behavior and corrosion inhibition of imidazoline inhibitors, *Iranian Journal of Chemistry and Chemical Engineering (IJCCE)*, 37(5):85-103 (2018).

[21] S. Elmi, Foroughi MM., Dehdab M., Shahidi-Zandi M., Computational evaluation of corrosion inhibition of four quinoline derivatives on carbon steel in aqueous phase, *Iranian Journal of Chemistry and Chemical Engineering (IJCCE),* 38(1):185-200 (2019).

[22] A.E Hassani, El Adnani Z., Benjelloun AT., Sfaira M., Mcharfi M., Benzakour M., Zarrouk A., Reactivity and Fe-complexation investigation by computational simulation studies on phenyltetrazole derivatives as mild steel corrosion inhibitors in aqueous acidic medium, *Journal of Molecular Liquids,* 349: 118169 (2022). M.E Belghiti, Echihi S., Mahsoune A., Karzazi Y., Aboulmouhajir A., Dafali A., Bahadur I., Piperine derivatives as green corrosion inhibitors on iron surface; DFT, Monte Carlo dynamics study and complexation modes, *Mol. Liq*., (2017). doi:10.1016/j.molliq.2018.03.127.

[23] T. A. Nyijime , H.F. Chahul, A. M. Ayuba, F. Iorhuna. Theoretical Investigations on Thiadiazole Derivatives as Corrosion Inhibitors on Mild Steel. *Adv. J. Chem. A*, 2023, 6(2), 141-154. https://doi.org/10.22034/AJCA.2023.383496.1352

[24] A.M Ayuba, T.A Nyijime, Theoretical study of 2-methyl benzoazole and its derivatives as corrosion inhibitors on aluminium metal surface, *J. Appl. Sci. Envir. Stud.* 4(2): 393-405 (2021).

[25] M. ElBelghiti M., Karzazi Y., Dafali A., Hammouti B., Bentiss F., Obot IB., Ebenso EE., Experimental, quantum chemical and Monte Carlo simulation studies of 3, 5-disubstituted-4-amino-1, 2, 4-triazoles as corrosion inhibitors on mild steel in acidic medium, *Journal of Molecular Liquids*, 218: 281-293 (2016).

[26] M.E Belghiti ME., Dafali A., Karzazi Y., Computational simulation and statistical analysis on the relationship between corrosion inhibition efficiency and molecular structure of some hydrazine derivatives in phosphoric acid on mild steel surface, *Applied Surface Science*, (2019). https://doi.org/10.1016/j.apsusc.2019.04.125.

[27] T.V Kumar TV., Makangara J., Laxmikanth C., Babu NS., Computational Studies for Inhibitory Action of2-Mercapto-1-Methylimidazole Tautomers on Steel Using of Density Functional Theory Method (DFT), *International Journal of Computational and Theoretical Chemistry*, 4(1): 1-6 (2016).

[28] S.J Smith SJ., Sutcliffe BT., The development of computational chemistry in the United Kingdom, *Review in computational chemistry*, 10: 271-316 (1972).

[29] I.B Obot, Gasem ZM., Umoren SA., Understanding the mechanism of 2-mercaptobenzimidazole adsorption on Fe (110), Cu (111) and Al (111) surfaces: DFT and molecular dynamics simulations approaches, *Int. J. Electrochem. Sci.* 9: 2367-2378 (2014).

[30] F.Iorhunaa, NA Thomas, SM Lawal. Theoretical properties of Thiazepine and its derivatives on inhibition of Aluminium *Al (110)* surface*. Alger. J. Eng. Technol. 2023*, 8(1) :43-51. DOI: https://doi.org/10.57056/ajet.v8i1.89

[31] W. Li W., Zhang Z., Zhai Y., Ruan L., Zhang W., Wu L., Corrosion Inhibition of N80 Steel by Newly Synthesized Imidazoline Based Ionic Liquid in 15% HCl Medium: Experimental and Theoretical Investigations, *International Journal of Electrochemical Science*, 15: 722–739 (2020).

[32] H. Lgaz, Saha SK., Chaouiki A., Bhat KS., Salghi R., Shubhalaxmi R., Banerjee P., Ali IH., Khan MI., Chung I., Evaluation of 2-Mercaptobenzimidazole Derivatives as Corrosion Inhibitors for Mild Steel in Hydrochloric Acid, *Construction and Building Materials*, 233: 117320 (2020).

[33] W.Kohn, Becke AD., Parr RG., Density functional theory of electronic structure, *The journal of physical chemistry*, 100(31):12974-12980 (1996).

[34] K.F Khaled, Abdel-Shafi NS., Al-Mobarak NA., Understanding Corrosion Inhibition of iron by 2-ThiophenecarboxylicAcid Methyl Ester: Electrochemical and Computational study, *Int. J. Electrochem. Sci*., 7: 1027 – 1044 (2012).

[35] F.Benhiba, Hsissou R., Abderrahim K., Serrar H., Rouifi Z., Boukhris S., Zarrouk A., Development of New Pyrimidine Derivative Inhibitor for Mild Steel Corrosion in Acid Medium, *Journal of Bio-and Tribo-Corrosion*, 8(2): 1-15 (2022).

[36] A.Thakur, Kaya S., Abousalem AS., Kumar A., Experimental, DFT and MC simulation analysis of Vicia Sativa weed aerial extract as sustainable and eco-benign corrosion inhibitor for mild steel in acidic environment, *Sustainable Chemistry and Pharmacy*, 29: 100785 (2022).

[37] T.W Quadri, Olasunkanmi LO., Fayemi OE., Lgaz H., Dagdag O., Sherif ESM., Ebenso EE., Computational insights into quinoxaline-based corrosion inhibitors of steel in HCl: Quantum chemical analysis and QSPR-ANN studies, *Arabian Journal of Chemistry*, 15(7): 103870 (2022).

[38] S. Donkor, Song Z., Jiang L., Chu H., An overview of computational and theoretical studies on analyzing adsorption performance of phytochemicals as metal corrosion inhibitors, *Journal of Molecular Liquids*, 119260 (2022).

[39] K.Adel, Hachani SE., Selatnia I., Nebbache N., Makhloufi S., Correlating the inhibitory action of novel benzimidazole derivatives on mild steel corrosion with DFT-based reactivity descriptors and MD simulations, *Journal of the Indian Chemical Society*, 99(7): 100497 (2022).

[40] N.Bhardwaj, Sharma P., Berisha A., Mehmeti V., Dagdag O., Kumar V., Monte Carlo simulation, molecular dynamic simulation, quantum chemical calculation and anti-corrosive behaviour of Citrus limetta pulp waste extract for stainless steel (SS-410) in acidic medium, *Materials Chemistry and Physics*, 284: 126052 (2022).

[41] S.A Mrani, Arrousse N., Haldhar R., Lahcen AA., Amine A., Saffaj T., Taleb M., In Silico approaches for some sulfa drugs as eco-friendly corrosion inhibitors of iron in aqueous medium, *Lubricants*, 10(3): 43 (2022).

[42] P.Geerlings, De Proft F., Chemical reactivity as described by quantum chemical methods, *International Journal of Molecular Sciences*, 3(4): 276-309 (2002).

[43] B. Gómez Likhanova NV., Domínguez-Aguilar MA., Martínez-Palou R., Vela A., Gázquez JL., Quantum chemical study of the inhibitive properties of 2-pyridyl-azoles, *J. Phys. Chem. B.*, 10(18): 8928-34 (2006).

[44] M.A Bedair, The effect of structure parameters on the corrosion inhibition effect of some heterocyclic nitrogen organic compounds, *J. Mol. Liq*., 219:128-41 (2016).

[45] I. Lukovits, Kalman E., Zucchi F., Corrosion inhibitors—correlation between electronic structure and efficiency, *Corrosion*, 57(1): 3-8 (2001).

[46] P.R Parr, Szentpály LV., Liu S., Electrophilicity index, *Journal of the American Chemical Society*, 121(9): 1922-1924 (1999).

[47] L.Guo, Safi ZS., Kaya S., Shi W., Tüzün B., Altunay N., Anticorrosive effects of some thiophene derivatives against the corrosion of iron: a computational study, *Front Chem*. 6:155 (2018).

[48] A.DehghaniS, Mostafatabar AH., Bahlakeh G., Detailed level computer modeling explorations complemented with comprehensive experimental studies of Quercetin as a highly effective inhibitor for acid-induced steel corrosion, *Journal of Molecular Liquids*, (2020). https://doi.org/10.1016/j.molliq.2020.113035.

[49] S. Joseph, John J., Electrochemical, quantum chemical, and molecular dynamic studies on the interaction of 4-amino-4H, 3,5-di(methoxy)-1,2,4-triazole (ATD), BATD and DBATD on copper metal in 1N H_2SO_4, *Materials and Corrosion*, 647: 625-632 (2013).

[50] S. Kaya, Ikot AN., Kumar A., Şimşek S., Zhu M., Guo L., Computational methods used in corrosion inhibition research, *In Eco-Friendly Corrosion Inhibitors*, 527-538 (2022).

[51] K. Lundgren, Effect of corrosion on the bond between steel and concrete: an overview, *Magazine of concrete research*, 59(6): 447-461 (2007).

[52] T. A. Nyijime, H. F. Chahul, A. M. Ayuba, F. Iorhuna. Theoretical Investigations on Thiadiazole Derivatives as Corrosion Inhibitors on Mild Steel. *Adv. J. Chem. A*, 6(2), 141-154 (2023).DOI:https://doi.org10.22034/AJCA.2023.383496.1352

[53] Delley, B. (2000) From Molecules to Solids with DMol3. Journal of Chemical Physics, 113, 7756-7764. https://doi.org/10.1063/1.1